

## RAPID REPORT | *Neural Circuits*

# Invariant and heritable local cortical organization as revealed by fMRI

Peka Christova<sup>1,2</sup> and Apostolos P. Georgopoulos<sup>1,2</sup>

<sup>1</sup>Department of Neuroscience, University of Minnesota Medical School, Minneapolis, Minnesota; and <sup>2</sup>Brain Sciences Center, Minneapolis Department of Veterans Affairs Health Care System, Minneapolis, Minnesota

Submitted 26 February 2018; accepted in final form 24 April 2018

**Christova P, Georgopoulos AP.** Invariant and heritable local cortical organization as revealed by fMRI. *J Neurophysiol* 120: 760–764, 2018. First published April 25, 2018; doi:10.1152/jn.00137.2018.—Neural interactions in local cortical networks critically depend on the distance between interacting elements: the shorter the distance, the stronger the interactions. Here we quantified these interactions in six cortical areas of 854 individuals, including monozygotic and dizygotic twins, nontwin siblings, and nonrelated individuals. We found that the strength of zero-lag correlation between prewhitened, resting-state, blood level oxygenation-dependent functional magnetic resonance imaging time series decreased with distance as a power law. The rate of decrease,  $b$ , varied among individuals by  $\sim 1.9\times$ , was highly correlated between hemispheres, but differed among areas (by  $\sim 1.2\times$ ) in a systematic fashion, becoming progressively less steep from frontal to occipital areas. With respect to twin status,  $b$  was significantly correlated between monozygotic twins, less so between dizygotic twins or nontwin siblings, and not at all in nonrelated individuals. These results quantify the lawful, distance-related cortical interactions and demonstrate, for the first time, the heritability of their power law.

**NEW & NOTEWORTHY** Local cortical circuitry involves orderly neuronal interactions. A key feature of these interactions is that they are stronger the closer the interacting neurons. Here we quantified this crucial dependence of neural interactions on distance with functional magnetic resonance imaging and found that the strength of interactions decreases with distance as a power law that is very similar in all cortical lobes and heritable. These findings identify an invariant and heritable property of local cortical organization.

cerebral cortex; fMRI; local cortical circuits

## INTRODUCTION

Neural interactions in local cortical networks critically depend on the distance between interacting elements (Georgopoulos and Stefanis 2010). Several anatomical studies in the monkey have shown that after a small, localized lesion in a cortical area fiber degeneration is dense for  $\sim 0.3$ – $0.5$  mm away from the lesion, whereas sparser degeneration extends up to several millimeters (Fisken et al. 1975; Gatter and Powell 1978; Huntley and Jones 1991; Shanks et al. 1978; Vogt and Pandya 1978). These findings suggest that neural interactions are strong in close vicinity and become weaker with increasing distance.

Address for reprint requests and other correspondence: A. P. Georgopoulos, Brain Sciences Center (11B), Department of Veterans Affairs Medical Center, One Veterans Dr., Minneapolis, MN 55417 (e-mail: omega@umn.edu).

Very little is known about these interactions in the human cerebral cortex. The advent of the Human Connectome Project (HCP, <https://www.humanconnectome.org>; Van Essen et al. 2013) has made such a study possible because of the high temporal (0.72 s) and spatial (2 mm isotropic) resolution of blood level oxygenation-dependent (BOLD) functional magnetic resonance imaging (fMRI) data acquisition (Uğurbil et al. 2013).

## MATERIALS AND METHODS

Data from the HCP 900 Subjects Data Release (December 8, 2015) were used in this study. Here we investigated distance-dependent interactions at rest in six cortical areas (superior frontal, precentral, postcentral, superior parietal, inferior parietal, lateral occipital) of 854 individuals [ $28.8 \pm 0.126$  yr old (mean  $\pm$  SE), range 22–37 yr; 480 women and 374 men], including 87 pairs of monozygotic (MZ) twins, 82 pairs of dizygotic (DZ) twins, 108 pairs of nontwin siblings (SIB), and 48 pairs of randomly paired nonrelated (NR) individuals. Interactions were assessed by calculating the zero-lag cross-correlation,  $r^0$ , between prewhitened (Blackman and Tukey 1959; Press and Tukey 1956) BOLD fMRI resting-state time series ( $n = 1,200$  time samples, every 0.72 s) recorded from vertices at all available distances from each other, within 12 mm (every 2 mm isotropic;  $n = \sim 2,000$  vertices per area). Each time series was prewhitened with an autoregressive integrative moving average (ARIMA) model (Box and Jenkins 1976) of orders ( $P = 15$ ,  $d = 1$ ,  $q = 1$ ) (Christova et al. 2011) yielding practically white noise innovations (Fig. 1); because of differencing ( $d = 1$  in ARIMA), the length on an innovations series was  $n = 1,199$ . Next, for each area, all zero-lag pairwise cross-correlations between innovations  $r^0$  were calculated. Altogether, 18,555,275,037  $r^0$  were calculated, corresponding to an average of 21,727,488 per brain ( $n = 854$  brains).

The  $r^0$  was  $z$ -transformed (Fisher 1958) to normalize its distribution and stabilize the variance for statistical analyses:

$$r_z^0 = \operatorname{atanh}(r^0) \quad (1)$$

Finally, for each vertex, all  $r_z^0$  for each distance (every 2 mm, up to 12 mm = 6 discrete distance values) were averaged, and those averages were further grand averaged for each area, hemisphere, and individual brain to obtain distance-related, average  $r_z^0$ . (The vascular lags over the 12-mm distances explored in the analysis are not expected to differ substantially, and hence the use of a zero-lag correlation is justified.) Altogether, there were 6 areas  $\times$  2 hemispheres  $\times$  6 distances  $\times$  854 brains = 61,488 such values available for analysis.

MATLAB (version 16, 2016) and IBM-SPSS (versions 23–25) were used to analyze the data. Standard statistical analyses included analysis of variance (ANOVA) and regression analysis. The intraclass

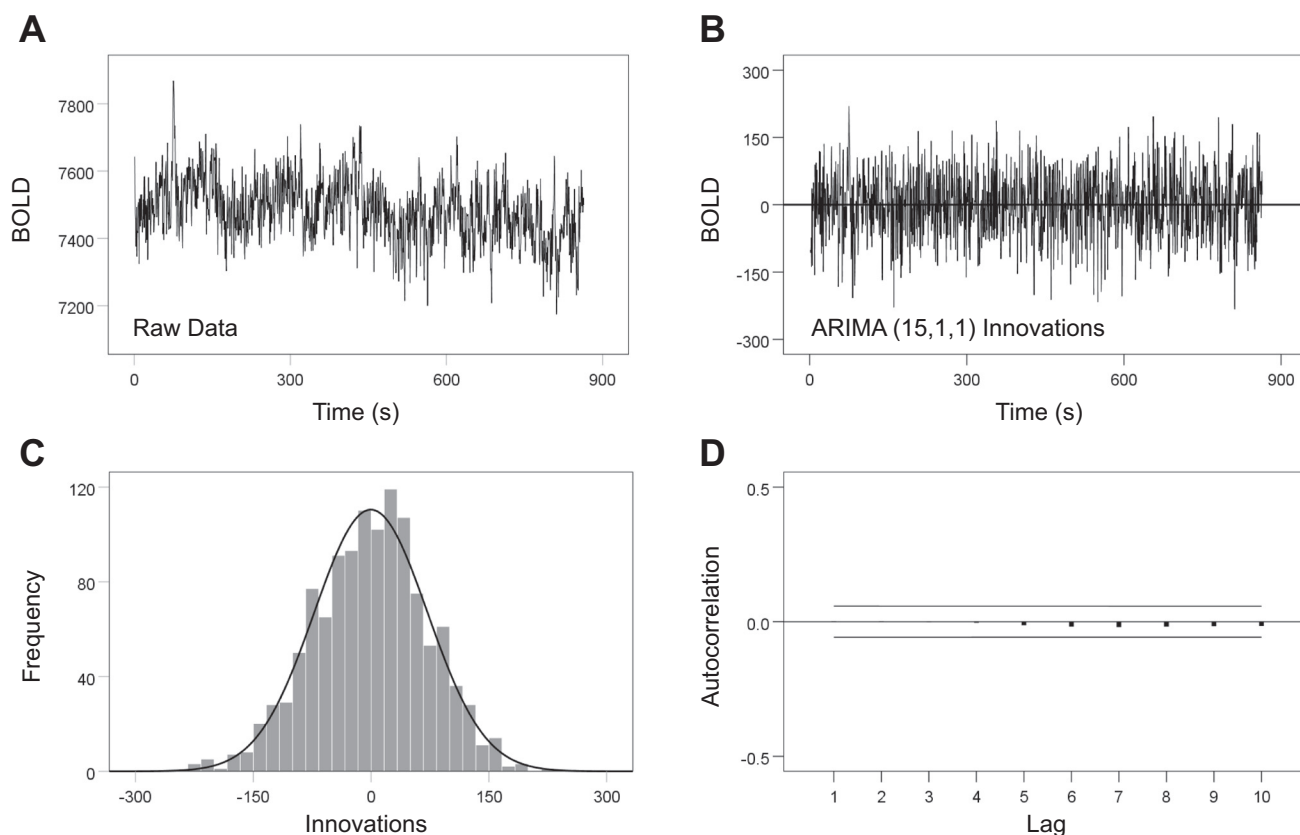


Fig. 1. The prewhitening of blood level oxygenation-dependent (BOLD) time series is illustrated for a single voxel in the precentral gyrus. *A*: time series of raw BOLD signal is plotted against time ( $n = 1,200$  time samples recorded every 0.72 s). *B*: innovations of the same series after prewhitening using an autoregressive integrative moving average (ARIMA) (15,1,1) model (see text for details). *C*: frequency distribution of the innovations with superimposed normal distribution curve. *D*: autocorrelation function of the innovations. *B–D* show that the raw BOLD series (*A*) was effectively prewhitened, i.e., the ARIMA (15,1,1) model yielded practically white noise innovations (residuals) that were independent and normally distributed with zero mean.

correlation was computed by the Reliability Procedure of SPSS, using a one-way random effects model (where people effects are random) and statistical significance for the conservative single measures. For statistical analyses across groups, the intraclass correlation was  $z$ -transformed (Fisher 1958) before the analyses.

## RESULTS

As a first, visualization step, we identified the connections within each area with  $r_z^0 > 0.5$  and plotted them color-coded (Fig. 2). This revealed an intricate pattern of internal connectivity that was not analyzed further. Instead, we assessed the change of  $r_z^0$  as a function of distance. We found that  $r_z^0$  decreased in an orderly fashion with distance  $D$ . The dependence of  $r_z^0$  on distance  $D$  followed a power law:

$$r_z^0 = kD^{-b} \quad (2)$$

where  $k$  is a constant and the exponent  $b$  quantifies the rate by which  $r_z^0$  declines with distance. An example is shown in Fig. 3A. Further analyses were conducted on 6 areas  $\times$  2 hemispheres  $\times$  854 brains = 10,248  $b$  values. We found the following: 1) The fit of the power law was excellent and very robust across areas (Fig. 3B). The overall ( $n = 10,248$ ) mean  $b$  was  $-1.33$  (SE = 0.016, SD = 0.162, median =  $-1.31$ ). 2) The exponent  $b$  was very similar between left and right hemispheres (Fig. 3C) but 3) varied systematically with the anteroposterior location of the area (Fig. 3D). Specifically, it

became less steep (i.e., less negative) from anterior to posterior (steepest in superior frontal, least steep in lateral occipital) (Fig. 3E).

Overall, the variation of  $b$  was largest among individuals (by  $1.9\times$  on average) and smallest among areas (by  $1.2\times$  on average). This is illustrated in Fig. 4, left, for two individuals with very different exponents: it can be seen that the difference in the exponents is maintained across the variation of the exponent in different areas. This finding suggests that the exponent  $b$  may be a characteristic feature of an individual brain, in which case it could be heritable. For that purpose, we first tested for the presence of a genetic component by calculating the intraclass correlation coefficient of  $b$  in four group pairs, namely, MZ twins ( $r_{MZ}$ ), DZ twins ( $r_{DZ}$ ), nontwin siblings ( $r_{SIB}$ ), and unrelated individuals ( $r_{NR}$ ). Indeed, we found a statistically significant positive intraclass correlation only for MZ, DZ, and SIB and not for NR, which did not differ significantly from zero (Fig. 4, right). Specifically, there were 6 areas  $\times$  2 hemispheres = 12 intraclass correlations for each group. For the MZ group, all  $r_{MZ}$  were highly statistically significant ( $P < 0.009$ ); for the DZ group, all  $r_{DZ}$  were statistically significant ( $P < 0.05$ ); for the SIB group, the 6  $r_{SIB}$  of the left hemisphere were statistically significant ( $P < 0.05$ ) but none of the right hemisphere; and for the NR group, none was statistically significant. Next, an ANOVA was used to compare  $z$ -transformed intraclass correlations (Fig. 4, right), with the following results: 1)  $r_{MZ}$  was significantly higher than

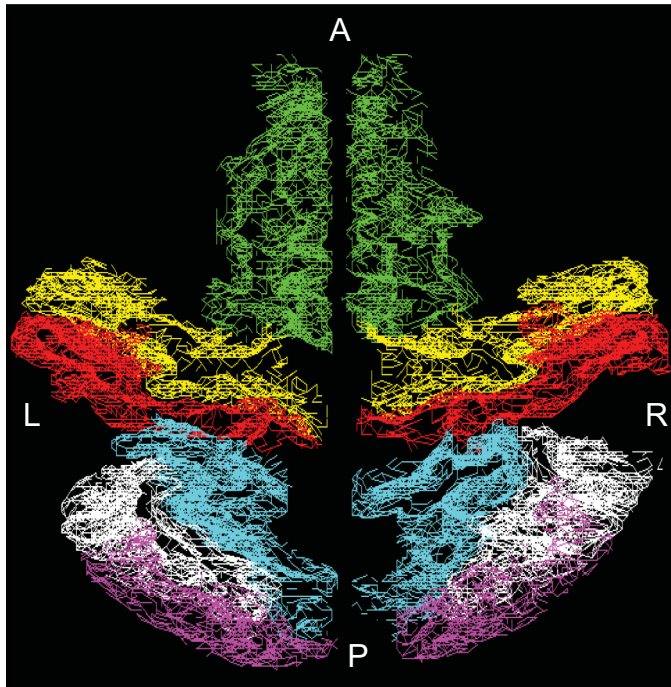


Fig. 2. Internal connectivity in 6 cortical areas; data from a single brain. A line connecting 2 vertices indicates  $r_z^0 > 0.5$ . A, anterior; P, posterior; M, medial; L, lateral. Areas from *top to bottom*: superior frontal gyrus (green), precentral gyrus (yellow), postcentral gyrus (red), superior parietal lobule (turquoise), inferior parietal lobule (white), lateral occipital gyrus (magenta). The probability value of  $r_z^0 > 0.5$  is  $P < 1 \times 10^{-50}$ , uncorrected for multiple comparisons. Given  $n = 1,200 - 1$  (because of differencing)  $- 15$  (because of 15 autoregressive orders) = 1,184 innovations, the SE of  $r_z^0$  (Fisher 1958) is  $SE = \frac{1}{\sqrt{N-3}} = \frac{1}{\sqrt{1,181}} = 0.029$ ; hence  $t_{[1181]} = \frac{0.5}{0.029} = 17.2$ ,  $P < 1 \times 10^{-50}$ . Given that a total of 21,727,488  $r_z^0$  were evaluated for this brain, the probability threshold for a (corrected)  $P = 0.001$  is  $P' = 0.001/21,727,488 = 4.6 \times 10^{-11}$ . Thus our threshold of  $P < 1 \times 10^{-50}$  is very conservative, even corrected for multiple comparisons.

$r_{DZ}$  ( $P = 0.014$ ),  $r_{SIB}$  ( $P = 0.001$ ), and  $r_{NR}$  ( $P < 10^{-12}$ ); 2)  $r_{DZ}$  was higher than but not statistically significantly different from  $r_{SIB}$  ( $P = 0.243$ ); and 3)  $r_{SIB}$  was significantly higher than  $r_{NR}$  ( $P < 10^{-7}$ ). Finally, we then calculated the heritability of  $b$ , using Falconer's formula (Falconer and Mackay 1996):

$$H_b^2 = 2(r_{MZ} - r_{DZ}) \quad (3)$$

Given  $r_{MZ} = 0.330$  and  $r_{DZ} = 0.236$ ,  $H_b^2 = 2(0.330 - 0.236) = 0.188$ .

## DISCUSSION

Several aspects of these findings are noteworthy. First, they are based on the temporal and spatial constraints of the fMRI acquisition protocol of the data analyzed, namely, a temporal synchronicity width of 0.72 s and a spatial resolution of 2 mm isotropic. These scales are larger than the typical neurophysiological (temporal) and neuroanatomical (spatial) scales. For example, the typical neurophysiological scale for neuronal spikes or local field potentials is 0.001 s, compared with which the BOLD temporal scale of 0.72 s is very large. However, the relevance of the temporal resolution is related to the specific application: although a high temporal resolution is essential for studying fast-evolving dynamic neural processes (e.g., during a

reaction time of a typical duration of 0.25 s), a low resolution may be adequate for no-task, resting-state conditions, such as the one in this study. With respect to the spatial resolution, a typical neuroanatomical scale in local cortical networks can extend from tens of micrometers (e.g., the width of a functional cortical column) to several millimeters (e.g., in topographical mapping studies). Therefore, the 2-mm resolution in this study is reasonable.

We found that local cortical networks in six different areas exhibit a robust distance-related dependence in their synchronicity, reflecting a local, spatial tuning. This dependence follows a power law, is specific for a given brain, and is heritable. In addition, it varies in a systematic fashion from anterior to posterior, as the drop in synchronicity becomes less sharp while moving toward more posterior areas. It is remarkable that very similar observations were made in the monkey by T. P. S. Powell and his colleagues in the 1970s (Fisken et al. 1975; Gatter and Powell 1978; Shanks et al. 1978) and by others (Huntley and Jones 1991; Vogt and Pandya 1978). It was found that after small localized lesions in the motor, somatosensory, or primary visual cortex fiber degeneration was dense for  $\sim 0.3$ – $0.5$  mm away from the lesion, whereas sparser degeneration extended up to several millimeters. These findings suggest that neural interactions are strong in close vicinity and become weaker with increasing distance. It is of special interest that Powell and colleagues also observed that the spread of fiber degeneration was longer in the visual cortex (5–6 mm; Fisken et al. 1975) than in the motor cortex (2–3 mm; Gatter and Powell 1978). This may relate to the functional specialization of the area. At face value, this extent of local cortical interactions within a few millimeters indicates an integrative cortical ensemble within which tangential, intercolumnar cortical operations take place, such as the neuronal population vector in the motor cortex (Georgopoulos et al. 2007; Naselaris et al. 2006a, 2006b), the integration of information across nearby receptive fields in the somatosensory cortex, and the hypercolumnar organization in the visual cortex. Remarkably, a power law with a very similar exponent of  $b = -1.5$  has been described for neuronal avalanches (Klaus et al. 2011). The systematic increase of the size of this postulated “canonical integrative cortical unit” from anterior to posterior suggests that integrative operations it subserves may involve increasingly larger local populations, a new aspect of cortical organization that remains to be elucidated.

## GRANTS

This study was supported by the American Legion Brain Sciences Chair, University of Minnesota. Data were provided by the Human Connectome Project, WU-Minn Consortium (Principal Investigators: David Van Essen and Kamil Ugurbil; 1U54MH091657) funded by the 16 National Institutes of Health (NIH) institutes and centers that support the NIH Blueprint for Neuroscience Research and by the McDonnell Center for Systems Neuroscience at Washington University.

## DISCLOSURES

No conflicts of interest, financial or otherwise, are declared by the authors.

## AUTHOR CONTRIBUTIONS

P.C. and A.P.G. conceived and designed research; P.C. and A.P.G. analyzed data; P.C. and A.P.G. interpreted results of experiments; P.C. and A.P.G.

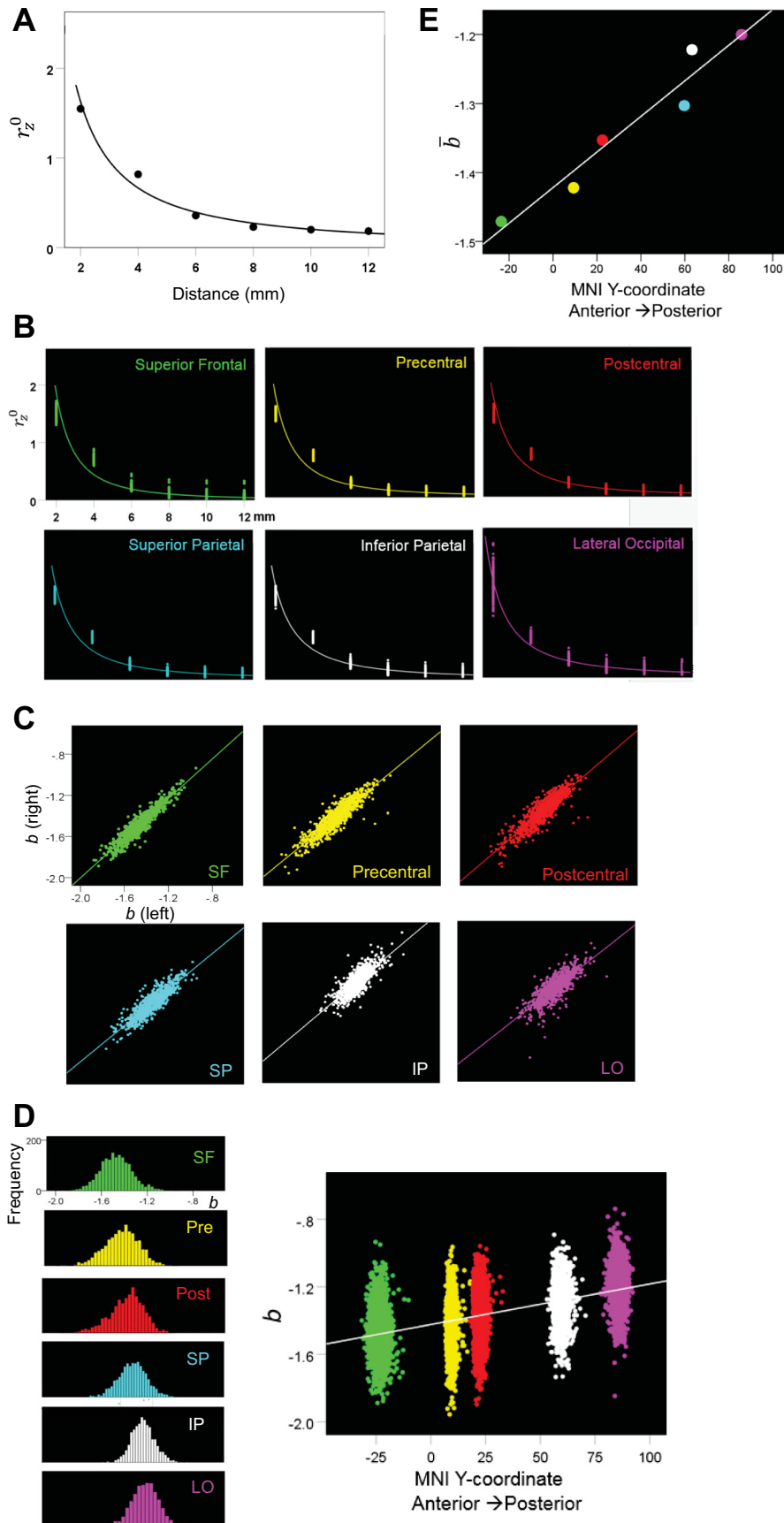
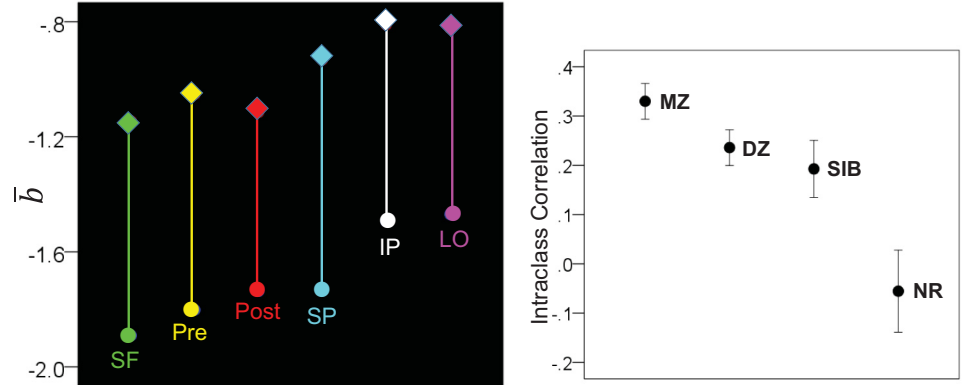


Fig. 3. Dependence of  $r_z^0$  on distance. *A*: mean  $r_z^0$  is plotted against distance. Data from a single subject, left precentral area. The line is a good power fit ( $R^2 = 0.964$ ,  $P < 0.0005$ ). *B*: power law functions for the 6 areas fitted on all subjects and hemispheres. Each cluster of filled circles contains 2 hemispheres  $\times$  854 brains = 1,708 points. Note the tight clustering of points and consistency of fitted power law functions [ $P < 10^{-50}$  for each plot, linear regression analysis;  $R^2 = 0.931, 0.929, 0.926, 0.938, 0.947, 0.949$  for superior frontal (SF), precentral (Pre), postcentral (Post), superior parietal (SP), inferior parietal (IP), and lateral occipital (LO) areas, respectively]. *C*: exponents  $b$  are plotted between the left and right hemispheres for each area ( $n = 854$  brains per plot). Note the high similarity of  $b$  between the 2 hemispheres ( $R^2 = 0.939, 0.901, 0.892, 0.890, 0.795, 0.787$  for SF, Pre, Post, SP, IP, and LO areas, respectively). *D, left*: frequency distribution of  $b$  for each area; all pairwise comparisons of  $b$  between areas were highly statistically significant ( $P$  ranged from  $P < 10^{-14}$  to  $P < 10^{-292}$ , Bonferroni adjusted for multiple comparisons, repeated-measures ANOVA with areas as within factors). *Right*: all  $b$  for each area are plotted against the anteroposterior coordinate of the Montreal Neurological Institute (MNI) atlas ( $R^2 = 0.317$ ,  $P < 10^{-50}$ ). *E*: the average  $\bar{b}$  per area is plotted against the average anteroposterior MNI coordinate ( $R^2 = 0.941$ ,  $P < 0.001$ ). The SEs of the points are too small ( $< 0.005$ ) to show.

Fig. 4. *Left*: average  $\bar{b}$  (per hemisphere) of 2 brains with very different  $b$  values are plotted for each area to illustrate the consistency of difference in  $\bar{b}$  across areas. SF, superior frontal; Pre, precentral; Post, postcentral; SP, superior parietal; IP, inferior parietal; LO, lateral occipital. *Right*: mean  $\pm$  SE (across areas and hemispheres) intraclass correlation of  $b$  for the 4 genetic groups of participants. The values for the nontwin sibling (SIB) and non-related (NR) groups are from a single random realization. One hundred random pairings of siblings (for the SIB group) and nonrelated participants (for the NR group) gave very similar values. MZ, monozygotic; DZ, dizygotic.



prepared figures; P.C. and A.P.G. drafted manuscript; P.C. and A.P.G. edited and revised manuscript; P.C. and A.P.G. approved final version of manuscript.

## REFERENCES

- Blackman RB, Tukey JW.** *The Measurement of Power Spectra from the Point of View of Communications Engineering.* New York: Dover, 1959.
- Box GE, Jenkins GM.** *Time Series Analysis: Forecasting and Control* (2nd ed.). San Francisco, CA: Holden-Day, 1976.
- Christova P, Lewis SM, Jerde TA, Lynch JK, Georgopoulos AP.** True associations between resting fMRI time series based on innovations. *J Neural Eng* 8: 046025, 2011. doi:10.1088/1741-2560/8/4/046025.
- Falconer DS, Mackay TF.** *Introduction to Quantitative Genetics* (4th ed.). Harlow, UK: Longmans Green, 1996.
- Fisher RA.** *Statistical Methods for Research Workers* (13th ed.). Edinburgh, UK: Oliver and Boyd, 1958.
- Fisken RA, Garey LJ, Powell TP.** The intrinsic, association and commissural connections of area 17 on the visual cortex. *Philos Trans R Soc Lond B Biol Sci* 272: 487–536, 1975. doi:10.1098/rstb.1975.0099.
- Gatter KC, Powell TP.** The intrinsic connections of the cortex of area 4 of the monkey. *Brain* 101: 513–541, 1978. doi:10.1093/brain/101.3.513.
- Georgopoulos AP, Merchant H, Naselaris T, Amirikian B.** Mapping of the preferred direction in the motor cortex. *Proc Natl Acad Sci USA* 104: 11068–11072, 2007. doi:10.1073/pnas.0611597104.
- Georgopoulos AP, Stefanis C.** The motor cortical circuit. In: *Brain Microcircuits*, edited by Shepherd G, Grillner S. New York: Oxford Univ. Press, 2010, p. 39–45. doi:10.1093/med/9780195389883.003.0005.
- Huntley GW, Jones EG.** Relationship of intrinsic connections to forelimb movement representations in monkey motor cortex: a correlative anatomic and physiological study. *J Neurophysiol* 66: 390–413, 1991. doi:10.1152/jn.1991.66.2.390.
- Klaus A, Yu S, Plenz D.** Statistical analyses support power law distributions found in neuronal avalanches. *PLoS One* 6: e19779, 2011. doi:10.1371/journal.pone.0019779.
- Naselaris T, Merchant H, Amirikian B, Georgopoulos AP.** Large-scale organization of preferred directions in the motor cortex. I. Motor cortical hyperacuity for forward reaching. *J Neurophysiol* 96: 3231–3236, 2006a. doi:10.1152/jn.00487.2006.
- Naselaris T, Merchant H, Amirikian B, Georgopoulos AP.** Large-scale organization of preferred directions in the motor cortex. II. Analysis of local distributions. *J Neurophysiol* 96: 3237–3247, 2006b. doi:10.1152/jn.00488.2006.
- Press H, Tukey JW.** *Flight Test Manual.* Neuilly sur Seine, France: NATO Advisory Group for Aeronautical Research and Development, 1956, chapter 1.41.
- Shanks MF, Pearson RC, Powell TP.** The intrinsic connections of the primary somatic sensory cortex of the monkey. *Proc R Soc Lond B Biol Sci* 200: 95–101, 1978. doi:10.1098/rspb.1978.0007.
- Uğurbil K, Xu J, Auerbach EJ, Moeller S, Vu AT, Duarte-Carvajalino JM, Lenglet C, Wu X, Schmitter S, Van de Moortele PF, Strupp J, Sapiro G, De Martino F, Wang D, Harel N, Garwood M, Chen L, Feinberg DA, Smith SM, Miller KL, Sotiropoulos SN, Jbabdi S, Andersson JL, Behrens TE, Glasser MF, Van Essen DC, Yacoub E; WU-Minn HCP Consortium.** Pushing spatial and temporal resolution for functional and diffusion MRI in the Human Connectome Project. *Neuroimage* 80: 80–104, 2013. doi:10.1016/j.neuroimage.2013.05.012.
- Van Essen DC, Smith SM, Barch DM, Behrens TE, Yacoub E, Ugurbil K; WU-Minn HCP Consortium.** The WU-Minn Human Connectome Project: an overview. *Neuroimage* 80: 62–79, 2013. doi:10.1016/j.neuroimage.2013.05.041.
- Vogt BA, Pandya DN.** Cortico-cortical connections of somatic sensory cortex (areas 3, 1 and 2) in the rhesus monkey. *J Comp Neurol* 177: 179–191, 1978. doi:10.1002/cne.901770202.